

Kinematic Model of Magnetic Domain Wall Motion for Fast, High-Accuracy Simulations

Kristi Doleh,^{1, a)} Leonard Humphrey,^{1, a)} Chandler M. Linseisen,¹ Michael D. Kitcher,² Joanna M. Martin,¹ Can Cui,³ Jean Anne C. Incorvia,³ Felipe Garcia-Sanchez,⁴ Naimul Hassan,¹ Alexander J. Edwards,¹ and Joseph S. Friedman¹

¹⁾*Electrical and Computer Engineering, The University of Texas at Dallas, Richardson, TX*

²⁾*Department of Materials Science & Engineering, Carnegie Mellon University, Pittsburgh, PA*

³⁾*Electrical and Computer Engineering, The University of Texas at Austin, Austin, TX*

⁴⁾*Departamento de Física Aplicada, Universidad de Salamanca, Salamanca, ES*

(*Electronic mail: Alexander.Edwards@utdallas.edu)

(*Electronic mail: Joseph.Friedman@utdallas.edu)

(*Electronic mail: fgs@usal.es)

(Dated: 4 June 2024)

Domain wall (DW) devices have garnered recent interest for diverse applications including memory, logic, and neuromorphic primitives; fast, accurate device models are therefore imperative for large-scale system design and verification. Extant DW motion models are sub-optimal for large-scale system design either over-consuming compute resources with physics-heavy equations or oversimplifying the physics, drastically reducing model accuracy. We propose a DW model inspired by the phenomenological similarities between motions of a DW and a classical object being acted on by forces like air resistance or static friction. Our proposed phenomenological model predicts DW motion within 1.2% on average compared with micromagnetic simulations that are 400 times slower. Additionally our model is seven times faster than extant collective coordinate models and 14 times more accurate than extant hyper-reduced models making it an essential tool for large-scale DW circuit design and simulation. The model is publicly posted along with scripts that automatically extract model parameters from user-provided simulation or experimental data to extend the model to alternative micromagnetic parameters.

Spintronic technologies have gained recent interest for use in memory and neuromorphic networks¹. Specifically, domain wall (DW) devices have been proposed for memory^{2,3} and logic³⁻⁵, as well as both synaptic⁶⁻⁸ and neuronal⁸⁻¹³ functions in level-based⁶ and spiking neural networks⁷⁻¹³. These proposals generally leverage the ability to move the DW through a spin-transfer torque (STT) or spin-orbit torque (SOT) current in a non-volatile manner and often electrically read the DW position using a magnetic tunnel junction (MTJ); the complete DW-MTJ can be treated as an electrical device and integrated directly into analog or digital circuits.

Proper design and verification of useful memory, logic, and neuromorphic network systems requires large-scale simulations. As simulating the full micromagnetic behavior of a large system comprising DW devices would require impractically large computational effort, compact device models with simplified physics are required. This can be challenging, as over-simplification of a device can lead to inaccurate simulation results, whereas overly complex models can contribute to exceedingly large simulation times.

Some previous DW models have been too simplistic, failing to account for some of the more non-linear aspects of DW motion^{14,15}. While these models may be useful for proof-of-concept simulations of circuits and systems, they are insufficiently accurate for designing and optimizing circuits that will

be implemented with real devices.

Other previous models, particularly those derived directly from equations like the Landau-Lifshitz-Gilbert (LLG) equation, have been overly complex. Very-high-accuracy DW models require a hybrid process that incorporates both a micromagnetic solver and a circuit simulator, requiring enormous computational resources²⁵⁻²⁷. Others have proposed the use of 1D or 2D collective coordinate (CC) models^{16-24,28}, which, while accounting for many of the observed phenomena, require more compute resources than necessary to accurately simulate. Furthermore, these models often do not match experimental data, relying so heavily on idealized equations that they become disconnected from practical devices. There thus does not exist a model that is both sufficiently fast and accurate for large-scale DW circuit simulations.

Critically, models derived from the LLG equation fail to take advantage of the strong similarities between the motion of a DW and a classical object, illustrated in Fig. 1. That is, one-dimensional DW motion resembles the kinematic motion of a classical object: both exhibit momentum, terminal velocity, and damping. By matching observed DW phenomena to their classical counterparts, DW acceleration can be deconstructed into component forces similar to an application of Newton's second law of motion.

Exploiting the similarities between the motion of a DW and classical object, we therefore propose the first DW model that accounts for observed non-linear phenomena while enabling extremely fast computation for large-scale simulation. We de-

^{a)}first authors contributed equally.

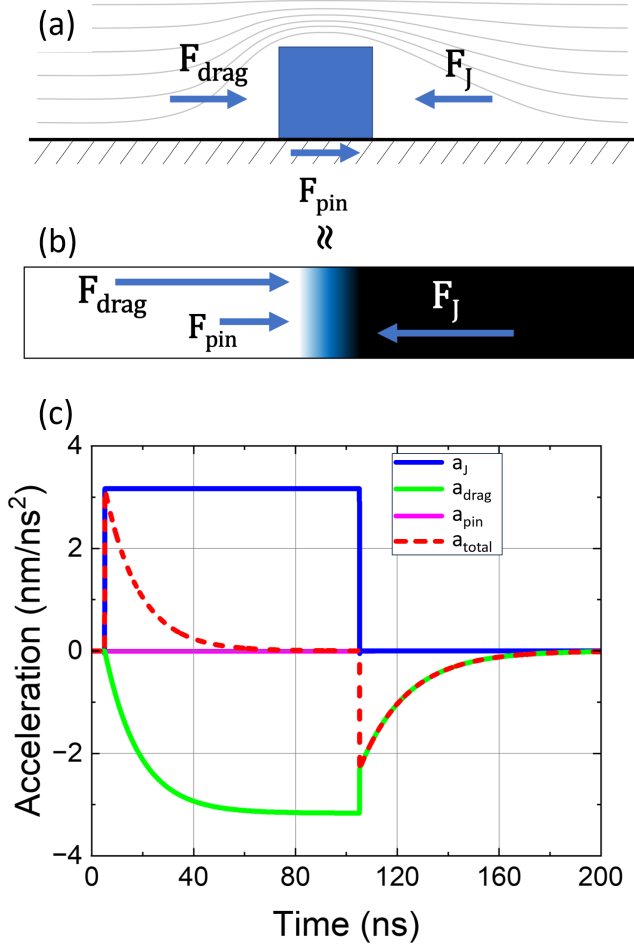


FIG. 1. (a) and (b) Free body diagram of DW motion for the proposed model alongside analogous classical system in which a box is pushed along a surface by a constant applied force through a viscous fluid. In this analogy, the current-induced force F_J is represented by the applied classical force, the micromagnetic damping force is represented by the fluid drag, and the DW pinning force is represented by the static friction when the box is resting. (c) The component accelerations of Equation 3 applied to the DW when a current pulse is applied and later removed. As the current density is sufficiently large, there is no pinning.

velop a low order kinematic model inspired by Stokes' drag equation:

$$\frac{d^2x}{dt^2} = -A * \frac{dx}{dt} + B \quad (1)$$

where the acceleration of the DW is a linear function of the velocity and the external forces, B. By fitting our low-order kinematic model to highly-accurate micromagnetic simulations, we achieve an ultra-low-cost yet sufficiently accurate model for simulating large DW networks that faithfully predicts the behavior of large-scale systems comprised of DW devices.

The model is verified against high-precision micromagnetic simulations across a wide range of micromagnetic parameters, faithfully predicting the DW position to within 1.2% on

average. The Verilog-A domain wall model is provided in the Supplementary Information and posted publicly at Github and our website along with automated scripts for extracting model parameters from user-provided micromagnetic simulation or experimental results, enabling effortless extension of the Verilog-A model to alternative micromagnetic parameters or stimuli.

In our proposed DW model, the DW is treated as an object in 1-dimensional space with continuous and differentiable position and velocity. A counterpart to Newton's second law can therefore be applied, expressing DW motion in terms of forces and resulting in a second-order ordinary differential equation for the DW velocity:

$$x''(t) = v'(t) = a(t) = a_J(t) + a_{damp}(t) + a_{pin}(t), \quad (2)$$

with

$$a_J(t) = \frac{F_J}{m}, \quad a_{damp} = \frac{F_{damp}}{m}, \quad a_{pin} = \frac{F_{pin}}{m}, \quad (3)$$

where x is the DW position, v is the DW velocity, a is the DW acceleration, m is the DW effective mass, a_J (F_J) is current-induced acceleration (force), a_{drag} (F_{drag}) is the damping acceleration (force), and a_{pin} (F_{pin}) is the pinning acceleration (force) when the DW is not moving. Figure 1 illustrates the proposed DW model alongside an analogous classical system. An argument from first principles justifying this second-order kinematic reduction is detailed in the Supplementary Information.

The component forces are based on classical counterparts and are modeled with polynomial fitting equations so as to closely match micromagnetic simulations. These fitting polynomials incorporate a number of micromagnetic parameters including effective mass, and are chosen to minimize model error relative to micromagnetic simulations. The model is trained on a range of micromagnetic and geometric parameter corners, leaving DW position as a hysteretic function of only current density and time. The model is reproduced in the Supplementary Information and posted publicly online along with scripts that automatically extract model fitting parameters from user-provided simulation or experimental data to extend the model beyond the 32 micromagnetic parameter corners evaluated here. The use of polynomial fitting functions as compared with the copious trigonometric evaluations required by conventional CC models provides our proposed model with a significant speedup with minimal loss in accuracy as demonstrated later in this work.

DW motion is stimulated using electrical current, applying a constant force to the DW. When a current is applied to the heavy metal layer of a DW device, DW motion is induced due to various micromagnetic effects including, but not limited to, SOT. This effective force – described by a_J – is a function of only the current density, J , and is therefore approximated with a quartic polynomial of J :

$$a_J = k_4 J^4 + k_3 J^3 + k_2 J^2 + k_1 J + k_0, \quad J \geq 0, \quad (4)$$

where $k_0 - k_4$ are fitting parameters. For $J < 0$, $a_J(J) = -a_J(-J)$, to ensure equal and opposite behavior for positive and negative current densities.

While this model has not been developed to incorporate STT or magnetic field stimuli, this kinematic DW model can be directly applied to such situations by solving for the appropriate model fitting terms with the approach described later in this work.

The damping force experienced by a DW limits the DW to a maximum velocity, as with an object moving through a viscous fluid. We model the damping as Stokes' drag: a force proportional to and opposing the velocity. As the magnitude of the damping changes with applied current density³¹, a linear function of J is incorporated in the model to account for this effect:

$$a_{damp} = -v * (d_1 + d_2|J|), \quad (5)$$

where d_1 and d_2 are fitting parameters. Under a constant applied current density, the DW accelerates until it reaches a terminal velocity when $a_J + a_{damp} = 0$. For a given micromagnetic parameter corner, this terminal velocity may be defined in terms of current density allowing k_0, \dots, k_4, d_1 , and d_2 to be determined simultaneously to closely match terminal velocity and acceleration time-constants extracted from the micromagnetic simulations.

DW pinning is modeled like static friction, such that if the DW is not moving, the pinning force will counter motion until the applied force is greater than a threshold. The force due to pinning is described by the following piecewise function:

$$F_{pin} = \begin{cases} -F_J, & |J| < p_1 \ \& \ |v| < p_2 \\ 0, & \text{otherwise} \end{cases} \quad (6)$$

where the thresholds p_1 and p_2 are tunable model parameters.

As the proposed kinematic model is 1-dimensional, track width is incorporated into the fitting parameters. Track length is a tunable parameter, and the DW is modeled to bounce off the track ends according to

$$v_{post_bounce} = -c_r * v_{pre_bounce}, \quad (7)$$

where the coefficient of restitution $c_r \in [0, 1]$ is a tunable model parameter.

Our kinematic model is demonstrated to be ultra-efficient with reasonably high accuracy compared with extant DW models. Micromagnetic simulations were used to glean model fitting parameters and benchmark accuracy. Our compact model was implemented in SPICE and simulated, demonstrating minimal deviation from micromagnetic simulation and significant speedup relative to hybrid micromagnetic models and CC models.

High-accuracy micromagnetic simulations were performed using mumax3 to develop and evaluate the model. As highlighted in Table I, DW track simulations were run across a large range of parameter corners to increase the application space of the model. These parameters include track width,

TABLE I. Micromagnetic parameters

| Parameter | Value(s) |
|---|---|
| Width [nm] | 50, 100 |
| Length [nm] | 500 |
| Thickness [nm] | 1.2 |
| Current Density (J) [mA/ μ m ²] | 8 to 800 |
| Saturation Magnetization (Msat) [A/m] | 7.95x10 ⁵ , 1.2x10 ⁶ |
| $B_{anis,eff}$ [mT] | 20, 350 |
| Anisotropy (Ku) [J/m ³] | 4.05x10 ⁵ , 5.36x10 ⁵ , 9.17x10 ⁵ , 1.11x10 ⁶ |
| Gilbert Damping Factor (α) | 0.01, 0.05 |
| Exchange stiffness (Aex) [J/m] | 11x10 ⁻¹² , 31x10 ⁻¹² |
| Current Pulse Width [ns] | 20 to 100 |

M_{sat} , $B_{anis,eff}$, α , and Aex , with Ku determined from M_{sat} and $B_{anis,eff}$ (further details are in the Supplementary Information).

Numerous training simulations were run across a dense range of current pulse densities J and pulse duration τ . The micromagnetic simulations comprised a DW in an infinitely long track stimulated by a single square current pulse of density J and duration τ . For each parameter corner, simulations were run over a range of ten current densities for a single pulse length, which was sufficiently long enough to perform model fitting for each corner.

Model parameters were chosen so as to minimize model error relative to DW position and velocity extracted from the micromagnetic simulations. For each micromagnetic parameter corner, a set of model fitting parameters is chosen to correctly predict DW motion for all of the simulated pulses with varying J and τ run on that parameter corner, and this process is detailed in the Supplementary Information. Therefore, for a single parameter corner, the model will be able to properly respond to a wide range of current pulses, including pulses of strange shapes. Through this process, we can therefore ensure our model remains accurate over a reasonable set of parameter combinations and input pulses. Additionally, the model may easily be extended to alternative micromagnetic parameters or stimuli, as described in the following paragraphs.

We have implemented the proposed kinematic DW model in Verilog-A, thereby enabling direct SPICE simulations of large-scale systems; this model is included in the Supplementary Information and posted publicly at Github and our website. Fitting parameters for the various parameter corners are left as model parameters that can be programmed by the user, and our table of inferred model fitting terms for each micromagnetic parameter corner is included in the Supplementary Information. While fitting parameters for parameter combinations not listed in the table may be interpolated from the existing data, future users should be aware that the model has only been verified against micromagnetic simulations at the listed parameter corners.

We have also supplied the scripts necessary should the reader wish to extend the model to a larger parameter space or alternate stimuli such as STT or magnetic field. The tem-

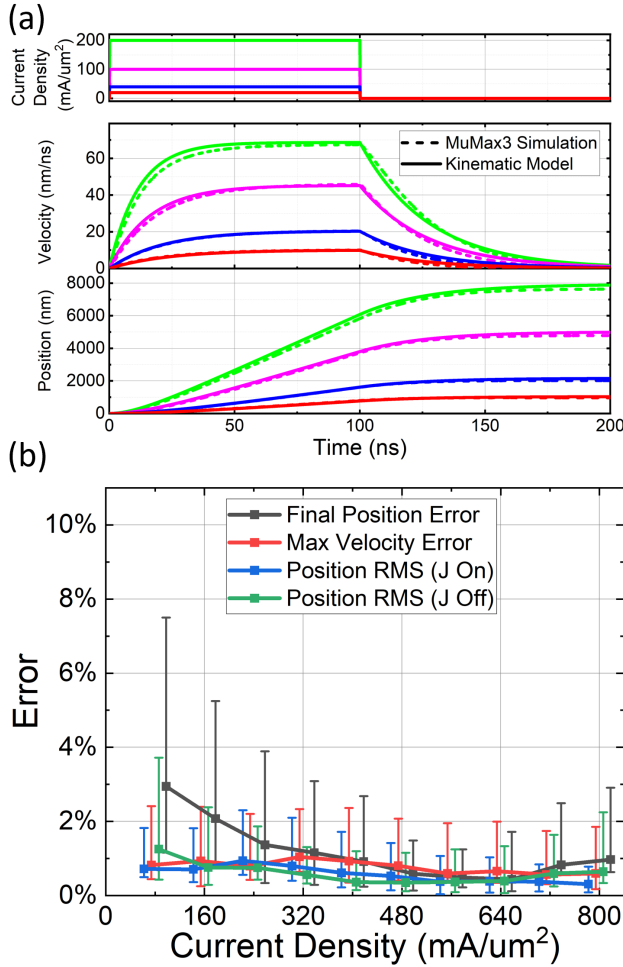


FIG. 2. (a) DW position in response to a current pulse, for both micromagnetic simulation and the kinematic model, with $A_{\text{ex}} = 11 \times 10^{-12}$ J/m, $K_{\text{u}} = 4.05 \times 10^5$ J/m³, $\alpha = 0.01$, $M_{\text{sat}} = 7.95 \times 10^5$ A/m, and track width = 100 nm. (b) Median, lower quartile, and upper quartile of four different error metrics averaged across tested values of all parameters.

plate mumax3 simulation script that is reproduced in the Supplementary Information and posted on Github and our website can be altered to match the desired parameter space or stimuli. Data should be collected across a range of stimuli strengths and pulse widths, and model fitting parameters can be automatically extracted using the Matlab scripts provided in the Supplementary Information and posted on Github and our website; the presented model is therefore flexible, with built-in mechanisms to assimilate new simulation or experimental data.

The kinematic DW model is directly amenable to DW-MTJ circuit simulations, though it is not limited to these applications; when used as a DW-MTJ, the modeled electrical behavior of the tunnel barrier is consistent with existing DW-MTJ models in the literature: it is modeled as a pair of parallel resistors, R_P and R_{AP} , according to:

$$R_{DW-MTJ} = \frac{R_P}{x} \left\| \frac{R_{AP}}{1-x} \right\|, \quad (8)$$

where x is the position of the DW normalized to the length of the track and R_P (R_{AP}) is the (anti-)parallel resistance of the device when $x = 1(0)$ ⁴. Track length, R_P , and R_{AP} are left as model parameters for the user.

For a single current pulse, the Verilog-A model matches very closely with the micromagnetic results across all parameter corners. Fig. 2(a) plots the DW position and velocity over time in response to various current densities for one of these parameter corners, highlighting the similarities between the kinematic model and mumax3 simulation.

The accuracy of the model was determined to be reasonably high across all reported parameter corners. Over each parameter corner, the accuracy of the model was analyzed using various error metrics including error in the final DW displacement, in the maximum velocity reached during the simulation, and the root mean square (RMS) error of the DW position over time. The error in the final DW position is most indicative of model performance for simulations with constant pulse width τ , whereas the error in maximum velocity is more indicative of model error when τ changes or is notably long, *i.e.* cases where the transient error would average out or become negligible. The RMS error in DW position was evaluated during the two transient periods of the simulation, the first being the time it took to reach maximum velocity and the second being the time it took to stop.

As illustrated in Figs. 2(b) and 3(a)-(e), the model demonstrates low error, < 1.2% on average. Fig. 3(a)-(e) depict the error averaged across the various values of all parameters except one which is held constant according to the figure caption. The model performs well in every case, though there are some parameter values where the model is more accurate; for instance, Fig. 3(b) illustrates that the model is more accurate with higher Gilbert damping.

Additionally, Fig. 3(f) shows high model performance at each parameter corner. For each corner, simulations were run with a range of ten values for J and a sufficiently large τ for the DW to reach its maximum velocity. In Fig. 3(f), the final position error, max velocity error, and RMS errors were averaged across all combinations of J and τ . The model performs exceptionally well at most parameter corners.

Furthermore, the kinematic Verilog-A model demonstrates close matching with more complicated current pulses, indicating the model will be very useful in analog simulations where DW devices are stimulated frequently. After model fitting, the model and the micromagnetic simulator were presented a complicated piecewise-constant input current signal as illustrated in Fig. 4(a) and Supplementary Movie 1. The model thus predicts DW position with very high accuracy compared with the micromagnetic simulation.

As illustrated in Fig. 4(b), the proposed kinematic DW model demonstrates significant speedup compared with CC models and significant accuracy boost compared with the oversimplifying models, making it very attractive for analog DW device network simulations. To enable this comparison,

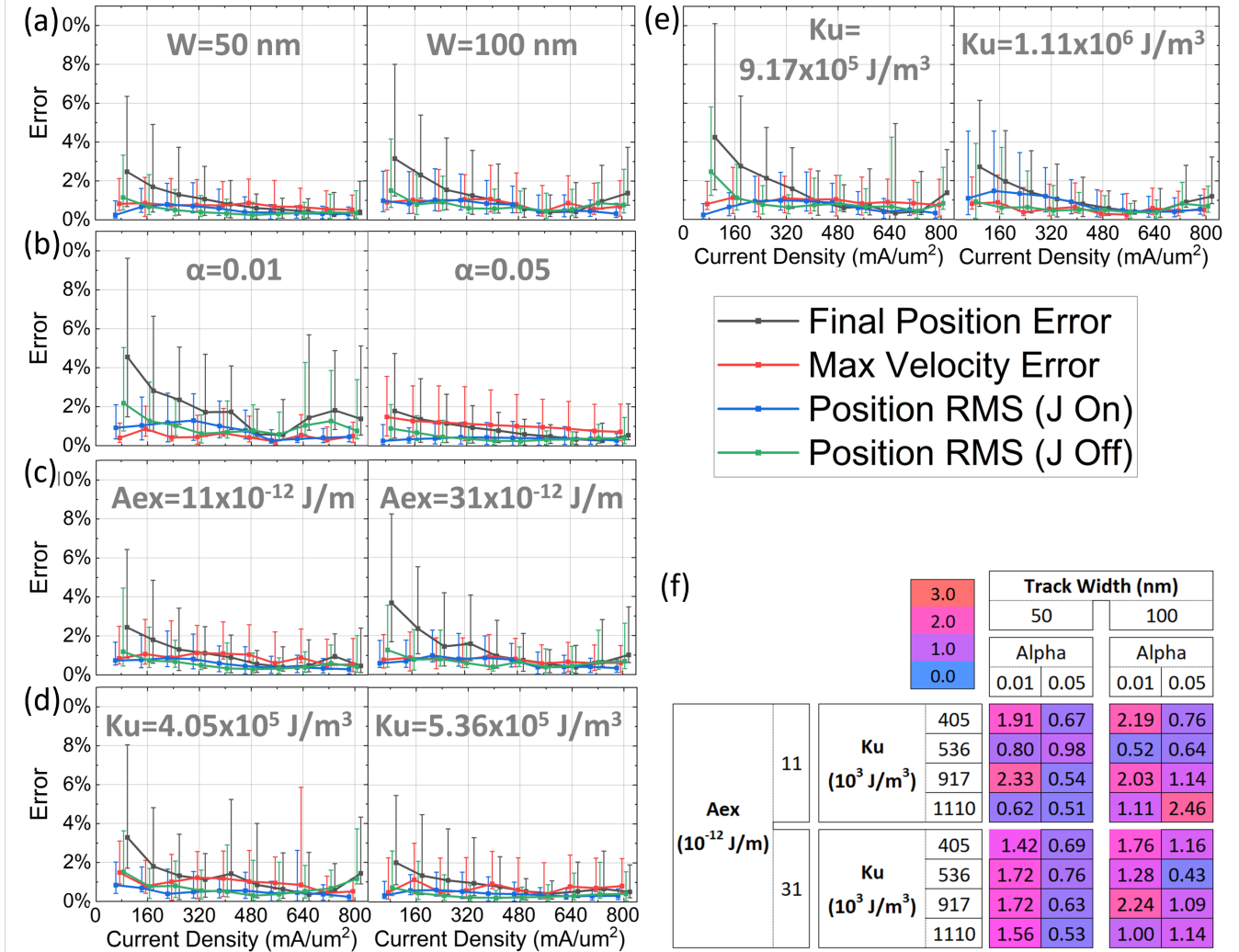


FIG. 3. (a) - (e) Median, lower quartile, and upper quartile of four different error metrics averaged across tested values of all parameters but one: α in (a), W in (b), A_{ex} in (c), and Ku in (d) and (e). (f) Averaged percent error over the ten runs of various current density J for each parameter corner simulated. In total this figure summarizes our model performance over 320 micromagnetic simulations.

the extant DW motion models were implemented in Python (see the Supplementary Information). For all of these models, both speedup and accuracy were evaluated relative to micromagnetic simulations as a baseline.

Compared with micromagnetic simulations, our proposed model presents a 400x speedup. This comes at a small accuracy cost of roughly 1.2% error, on average. Compared with CC models, our model presents an 7x speedup, with minimal accuracy loss compared with the best CC models.

Finally, our model demonstrates very large accuracy boost compared with the oversimplifying models of^{4,14}, with an acceptable 50% loss in speed. This drastic increase in accuracy is due to the inclusion of non-linear terms which the models of^{4,14} do not use.

In this work, we present a DW model inspired by the phenomenological similarities between a DW and a classical object subject to Newton's second law of motion. The model is posted publicly online along with scripts to automatically

extract model fitting parameters from new simulation or experimental data. Over the 32 parameter corners tested in this work, our proposed phenomenological model predicts DW motion within 1.2% on average compared with micromagnetic simulations. The model is two orders of magnitude faster than micromagnetic simulations, significantly faster than CC models, and drastically more accurate than overly reductive models. We therefore anticipate that our proposed kinematic model will significantly advance the simulation and design of large-scale networks of DW devices for digital, analog, and neuromorphic applications.

REFERENCES

- ¹J. Grollier, D. Querlioz, and M. D. Stiles, "Spintronic nanodevices for bioinspired computing," *Proceedings of the IEEE*, vol. 104, no. 10, pp. 2024–2039, 2016.

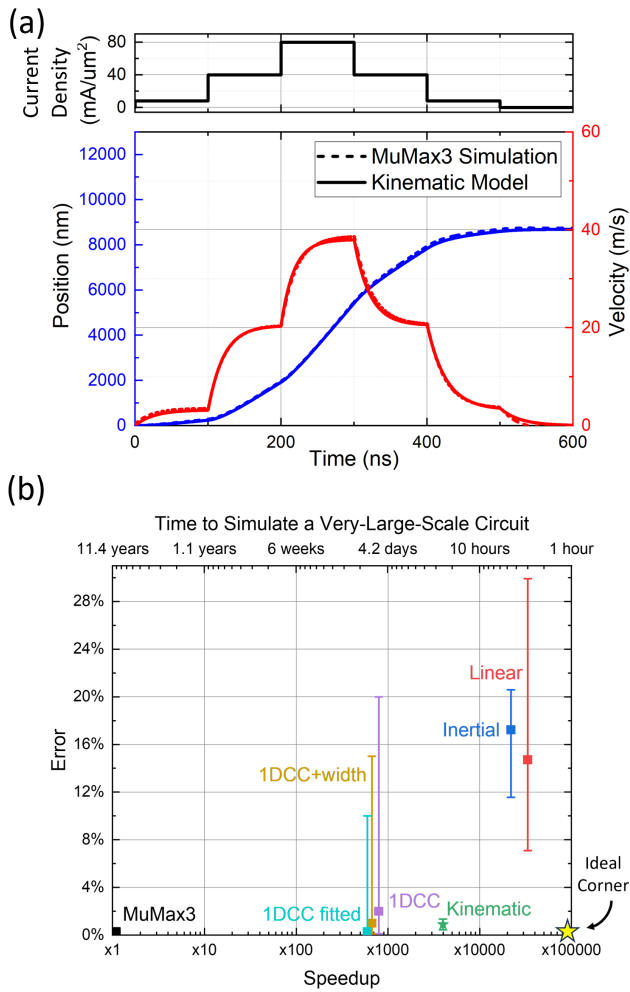


FIG. 4. (a) Predictive nature of model for complex input sequences, with $A_{ex} = 11 \times 10^{-12}$, $K_u = 4.05 \times 10^5$, $\alpha = 0.01$, $M_{sat} = 7.95 \times 10^5$, and track width = 100×10^{-9} . (b) Model accuracy and speedup compared relative to previously published work. Python implementations of the linear model¹⁴, inertial model¹⁵, kinematic model (this work), 1D CC model with and without variable wall width¹⁶, and 1D CC model with fitting parameters²³ are compared. Speedup is normalized relative to the mumax3 simulations. Time to simulate a very-large-scale circuit is normalized to one hour.

²S. S. P. Parkin, M. Hayashi, and L. Thomas, “Magnetic domain-wall race-track memory,” *Science*, vol. 320, no. 5873, pp. 190–194, 2008.

³M. Alamdar, T. Leonard, C. Cui, B. P. Rimal, L. Xue, O. G. Akinola, T. Patrick Xiao, J. S. Friedman, C. H. Bennett, M. J. Marinella, and J. A. C. Incorvia, “Domain wall-magnetic tunnel junction spin-orbit torque devices and circuits for in-memory computing,” *Applied Physics Letters*, vol. 118, no. 11, p. 112401, 2021.

⁴X. Hu, A. Timm, W. H. Brigner, J. A. C. Incorvia, and J. S. Friedman, “Spice-only model for spin-transfer torque domain wall mtj logic,” *IEEE Transactions on Electron Devices*, vol. 66, no. 6, pp. 2817–2821, 2019.

⁵T. P. Xiao, C. H. Bennett, X. Hu, B. Feinberg, R. Jacobs-Gedrim, S. Agarwal, J. S. Brunhaver, J. S. Friedman, J. A. C. Incorvia, and M. J. Marinella, “Energy and performance benchmarking of a domain wall-magnetic tunnel junction multibit adder,” *IEEE Journal on Exploratory Solid-State Computational Devices and Circuits*, vol. 5, no. 2, 2019.

⁶S. Liu, T. P. Xiao, C. Cui, J. A. C. Incorvia, C. H. Bennett, and M. J. Marinella, “A domain wall-magnetic tunnel junction artificial synapse with

notched geometry for accurate and efficient training of deep neural networks,” *Applied Physics Letters*, vol. 118, no. 20, p. 202405, 2021.

⁷K. Yue, Y. Liu, R. K. Lake, and A. C. Parker, “A brain-plausible neuromorphic on-the-fly learning system implemented with magnetic domain wall analog memristors,” *Science Advances*, vol. 5, no. 4, p. eaau8170, 2019.

⁸O. Akinola, X. Hu, C. H. Bennett, M. Marinella, J. S. Friedman, and J. A. C. Incorvia, “Three-terminal magnetic tunnel junction synapse circuits showing spike-timing-dependent plasticity,” *Journal of Physics D: Applied Physics*, vol. 52, no. 49, p. 49LT01, sep 2019. [Online]. Available: <https://doi.org/10.1088/1361-6463/ab4157>

⁹N. Hassan, X. Hu, L. Jiang-Wei, W. H. Brigner, O. G. Akinola, F. Garcia-Sanchez, M. Pasquale, C. H. Bennett, J. A. C. Incorvia, and J. S. Friedman, “Magnetic domain wall neuron with lateral inhibition,” *Journal of Applied Physics*, vol. 124, no. 15, p. 152127, 2018.

¹⁰W. H. Brigner, X. Hu, N. Hassan, C. H. Bennett, J. A. C. Incorvia, F. Garcia-Sanchez, and J. S. Friedman, “Graded-anisotropy-induced magnetic domain wall drift for an artificial spintronic leaky integrate-and-fire neuron,” *IEEE Journal on Exploratory Solid-State Computational Devices and Circuits*, vol. 5, no. 1, pp. 19–24, 2019.

¹¹C. Cui, O. G. Akinola, N. Hassan, C. H. Bennett, M. J. Marinella, J. S. Friedman, and J. A. C. Incorvia, “Maximized lateral inhibition in paired magnetic domain wall racetracks for neuromorphic computing,” *Nanotechnology*, vol. 31, no. 29, p. 294001, may 2020. [Online]. Available: <https://doi.org/10.1088/1361-6528/ab86e8>

¹²W. H. Brigner, N. Hassan, X. Hu, C. H. Bennett, F. Garcia-Sanchez, C. Cui, A. Velasquez, M. J. Marinella, J. A. C. Incorvia, and J. S. Friedman, “Domain wall leaky integrate-and-fire neurons with shape-based configurable activation functions,” *IEEE Transactions on Electron Devices*, vol. 69, no. 5, 2022.

¹³A. Agrawal and K. Roy, “Mimicking leaky-integrate-fire spiking neuron using automation of domain walls for energy-efficient brain-inspired computing,” *IEEE Transactions on Magnetics*, vol. 55, no. 1, pp. 1–7, 2019.

¹⁴W. S. Zhao, J. Duval, D. Ravelosona, J.-O. Klein, J. V. Kim, and C. Chappert, “A compact model of domain wall propagation for logic and memory design,” *Journal of Applied Physics*, vol. 109, no. 7, p. 07D501, 2011.

¹⁵X. Hu, A. J. Edwards, T. P. Xiao, C. H. Bennett, J. A. C. Incorvia, M. J. Marinella, and J. S. Friedman, “Process variation model and analysis for domain wall-magnetic tunnel junction logic,” in *2020 IEEE International Symposium on Circuits and Systems (ISCAS)*, 2020, pp. 1–5.

¹⁶M. Wang and Y. Jiang, “Compact model of domain wall mtj driven by spin orbit torque and dzyaloshinskii–moriya interaction,” *IEEE Transactions on Magnetics*, pp. 1–1, 2021.

¹⁷A. Thiaville and Y. Nakatani, *Domain-Wall Dynamics in Nanowires and Nanostrips*. Berlin, Heidelberg: Springer Berlin Heidelberg, 2006, pp. 161–205.

¹⁸D. G. Porter and M. J. Donahue, “Velocity of transverse domain wall motion along thin, narrow strips,” *Journal of Applied Physics*, vol. 95, no. 11, p. 6729–6731, 2004.

¹⁹A. Thiaville, Y. Nakatani, J. Miltat, and N. Vernier, “Domain wall motion by spin-polarized current: a micromagnetic study,” *Journal of Applied Physics*, vol. 95, no. 11, pp. 7049–7051, 2004.

²⁰A. Thiaville, J. García, and J. Miltat, “Domain wall dynamics in nanowires,” *Journal of Magnetism and Magnetic Materials*, vol. 242–245, pp. 1061–1063, 2002, proceedings of the Joint European Magnetic Symposia (JEMS’01). [Online]. Available: <https://www.sciencedirect.com/science/article/pii/S0304885301013531>

²¹X.-g. Wang, G.-h. Guo, Y.-z. Nie, G.-f. Zhang, and Z.-x. Li, “Domain wall motion induced by the magnonic spin current,” *Phys. Rev. B*, vol. 86, p. 054445, Aug 2012. [Online]. Available: <https://link.aps.org/doi/10.1103/PhysRevB.86.054445>

²²E. Martínez, S. Emori, N. Perez, L. Torres, and G. S. D. Beach, “Current-driven dynamics of dzyaloshinskii domain walls in the presence of in-plane fields: Full micromagnetic and one-dimensional analysis,” *Journal of Applied Physics*, vol. 115, no. 21, p. 213909, 2014.

²³C. Wang, Z. Wang, M. Wang, X. Zhang, Y. Zhang, and W. Zhao, “Compact model of dzyaloshinskii domain wall motion-based mtj for spin neural networks,” *IEEE Transactions on Electron Devices*, vol. 67, no. 6, pp. 2621–2626, 2020.

²⁴L. Thevenard, C. Gourdon, S. Haghgoo, J.-P. Adam, H. J. von Bardeleben, A. Lemaître, W. Schoch, and A. Thiaville, “Domain wall propagation

- in ferromagnetic semiconductors: Beyond the one-dimensional model,” *Phys. Rev. B*, vol. 83, p. 245211, Jun 2011. [Online]. Available: <https://link.aps.org/doi/10.1103/PhysRevB.83.245211>
- ²⁵J. A. Currivan, Y. Jang, M. D. Mascaro, M. A. Baldo, and C. A. Ross, “Low energy magnetic domain wall logic in short, narrow, ferromagnetic wires,” *IEEE Magnetics Letters*, vol. 3, pp. 3 000 104–3 000 104, 2012.
- ²⁶A. Roohi, R. Zand, and R. F. DeMara, “A tunable majority gate-based full adder using current-induced domain wall nanomagnets,” *IEEE Transactions on Magnetics*, vol. 52, no. 8, pp. 1–7, 2016.
- ²⁷C. Augustine, A. Raychowdhury, B. Behin-Aein, S. Srinivasan, J. Tschanz, V. K. De, and K. Roy, “Numerical analysis of domain wall propagation for dense memory arrays,” in *2011 International Electron Devices Meeting*, 2011, pp. 17.6.1–17.6.4.
- ²⁸S. A. Nasser, E. Martinez, and G. Durin, “Collective coordinate descriptions of magnetic domain wall motion in perpendicularly magnetized nanostructures under the application of in-plane fields,” *Journal of Magnetism and Magnetic Materials*, vol. 468, pp. 25–43, 2018. [Online]. Available: <https://www.sciencedirect.com/science/article/pii/S0304885318309259>
- ²⁹A. P. Malozemoff and J. C. Slonczewski, *Magnetic domain walls in bubble materials*. Academic Press, 1979.
- ³⁰S. Emori, U. Bauer, S.-M. Ahn, E. Martinez, and G. S. Beach, “Current-driven dynamics of chiral ferromagnetic domain walls,” *Nature materials*, vol. 12, no. 7, pp. 611–616, 2013.
- ³¹J. Torrejon, E. Martinez, and M. Hayashi, “Tunable inertia of chiral magnetic domain walls,” *Nature Communications*, vol. 7, no. 1, p. 13533, Nov 2016.
- ³²O. Boulle, S. Rohart, L. D. Buda-Prejbeanu, E. Jué, I. M. Miron, S. Pizzini, J. Vogel, G. Gaudin, and A. Thiaville, “Domain wall tilting in the presence of the dzyaloshinskii-moriya interaction in out-of-plane magnetized magnetic nanotracks,” *Phys. Rev. Lett.*, vol. 111, p. 217203, Nov 2013. [Online]. Available: <https://link.aps.org/doi/10.1103/PhysRevLett.111.217203>
- ³³P. Géhanne, A. Thiaville, S. Rohart, and V. Jeudy, “Chiral magnetic domain walls under transverse fields: A semi-analytical model,” *Journal of Magnetism and Magnetic Materials*, vol. 530, p. 167916, July 2021. [Online]. Available: <https://www.sciencedirect.com/science/article/pii/S030488532100192X>
- ³⁴S. Moretti, M. Voto, and E. Martinez, “Dynamical depinning of chiral domain walls,” *Phys. Rev. B*, vol. 96, p. 054433, Aug 2017. [Online]. Available: <https://link.aps.org/doi/10.1103/PhysRevB.96.054433>